

Thermal Residual Stresses in Freely Quenched Slabs of Semicrystalline Polymers: Simulation and Experiment

X. GUO,* A. I. ISAYEV

Institute of Polymer Engineering, The University of Akron, Akron, Ohio 44325-0301

Received 6 May 1999; accepted 26 August 1999

ABSTRACT: Thermal residual stresses in freely quenched semicrystalline polymer slabs were calculated based upon the modifications of the Indenbom theory for inorganic glasses and linear viscoelasticity. These modifications were introduced to include the influences of crystallization on mechanical and physical properties of the polymer during free quenching. The nonisothermal crystallization kinetic model due to Nakamura et al. was employed to calculate the variations of crystallinity. In the case of the Indenbom theory, a polymer during crystallization was assumed to undergo an abrupt transition from an ideal plastic state to an elastic state upon the completion of crystallization. In the case of linear viscoelasticity, the Morland–Lee constitutive equation was utilized with the effect of crystallization on the time–temperature dependent shear relaxation modulus taken into account. The Spencer–Gilmore $P - V - T$ equation of state was employed to model the specific volume changes during crystallization and used to determine the local thermal loading that results from inhomogeneous densifications and gives rise to the thermal residual stresses in the slabs. Based on the above theoretical work, the thermoelastic and thermoviscoelastic models were developed, and the corresponding numerical simulation schemes were formulated to calculate the residual thermal stresses in freely quenched slabs of semicrystalline polymers. Free quenching experiments were carried out under various cooling conditions using isotactic polypropylene. The layer removal method due to Treuting and Read was utilized to measure the residual thermal stresses. The simulated and measured results were then compared. The effects of quenching conditions and crystallization on the development of residual thermal stresses were evaluated. It has been found that both coolant types and coolant temperature have significant effects on residual thermal stresses. In contrast, initial temperature of the polymer melt shows a slight influence only. © 2000 John Wiley & Sons, Inc. *J Appl Polym Sci* 75: 1404–1415, 2000

Key words: residual stresses; thermal stresses; free quenching; semicrystalline polymer; isotactic polypropylene; crystallization; shear relaxation modulus; linear viscoelasticity

INTRODUCTION

Residual stresses are the stresses that exist in a material free of external load. They generally result from nonhomogeneous plastic deformation

inside the material, which is introduced by different sources. Molded polymeric products contain some amount of frozen-in residual stresses due to the changes in mechanical and physical properties under nonisothermal flow and inhomogeneous cooling during polymer processing operations.^{1,2} Such stresses can be attributed to two main resources. The one is due to the shear and normal stresses that develop during nonisothermal flow. These flow stresses do not completely

Correspondence to: A. I. Isayev (aisayev@uakron.edu).

* Present address: Daig Division, St. Jude Medical Inc., 14901 DeVeau Place, Minnetonka, MN 55345.

Journal of Applied Polymer Science, Vol. 75, 1404–1415 (2000)

© 2000 John Wiley & Sons, Inc.

CCC 0021-8995/00/111404-12

relax but get frozen-in due to rapid cooling. The other is due to the effects arising from nonisothermal cooling. The latter results in inhomogeneous densification inside the polymer and the changes in viscoelastic properties of the polymer. As a result, thermally induced local plastic deformation in terms of thermal loading would be introduced between the elements of materials. Thus, thermal stresses develop as the cooling progresses. Such stresses become residual when the polymer vitrifies. In this article, we limit ourselves to a study of the residual thermal stresses, as presented in freely quenched polymer slabs only.

It is well recognized that residual stresses strongly affect the end-use properties and warpage of polymeric products. Considerable reduction in the amount of frozen-in stresses and molecular orientation reduces the tendency of the moldings to "craze" and improves their dimensional stability on heating. It is hoped that an accurate prediction of residual stresses will allow one to determine optimum processing conditions. Thus, the factors governing the development of residual stresses during polymer processing have received much attention among many researchers over the years. However, these are concerned mainly with amorphous polymers, such as polystyrene, polycarbonate, and poly(methyl methacrylate).¹⁻¹⁷ For semicrystalline polymers like polyethylene and isotactic polypropylene, the relevant research work is rarely seen.^{18,19} This is because the mechanism for the formation of thermal stresses is greatly complicated by the accompanying crystallization during processing. Unlike an amorphous polymer whose thermal stresses arise due to the passage through its glass transition temperature T_g during cooling, thermal stresses in a semicrystalline polymer are present due to the occurrence of crystallization.¹⁹

Relevant theoretical works on the thermal stresses in quenched amorphous polymers are generally originated from those for inorganic glasses. Isayev¹ and Isayev and Crouthamel² have given a review on the subject. Roughly speaking, the theories can be broken down into two categories. One is based upon the instant freezing assumption.^{1,2,20,21} It states that at a temperature well above a glass transition temperature T_g , the polymer can be treated as an idealized fluid, bearing no stresses due to the relatively low shear modulus. Below T_g , the polymer is solidified, behaving like an idealized elastic material. The other is based upon the free volume relaxation assumption^{1,2,7,9,16,17,22-27} to take into account the time- and temperature-dependence of

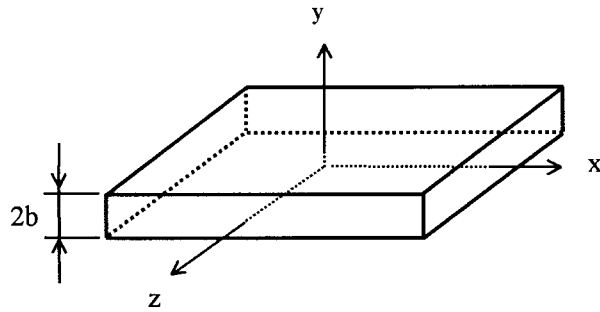
shear relaxation modulus of the polymer during quenching. An appropriate viscoelastic constitutive equation relating the stresses to the strains of the polymer has to be included in this case. There exist many versions of the equation. However, the one derived by Morland and Lee²² seems to be of the most appealing to many researchers, including Kabanemi and Crochet,⁷ Shyu and Isayev,⁹ Muki and Sternberg,²³ Lee and Rogers and Lee et al.,^{24,25} Narayanaswamy and Gardon,²⁶ and Narayanaswamy.²⁷ They utilized the Morland–Lee viscoelastic constitutive equation to calculate residual thermal stresses in inorganic or polymeric glasses. Apparently, the theoretical models for the calculation of residual thermal stresses in amorphous polymer cannot be immediately applied for the cases of semicrystalline polymers. However, it is noted that the mechanical and physical properties of semicrystalline polymers experience a similar transition upon the occurrence of crystallization.

In the present article, we pose a typical problem for the free quenching of semicrystalline polymers in an attempt to develop the models and study the effects of crystallization on the development of residual thermal stresses. Both the instant freezing and free volume relaxation assumptions for inorganic glasses and amorphous polymers are utilized. Based on the modifications of the Indenbom theory²¹ and linear viscoelasticity²² with crystallization phenomena taken into account, the thermoelastic model (ThEM) and thermoviscoelastic model (ThVEM) for the calculation of thermal stresses in symmetrically cooled slabs of isotactic polypropylenes are developed, respectively. The numerical schemes for solving the models are then formulated using a finite difference method. To verify the modeling, free quenching experiments are conducted under various cooling conditions using a typical semicrystalline polymer, namely, isotactic polypropylene. By employing the layer removal method,²⁸ residual thermal stresses in freely quenched i-PP slabs are measured and compared with model predictions. The effects of quenching conditions and crystallization on the formation of residual thermal stresses in semicrystalline polymers are evaluated.

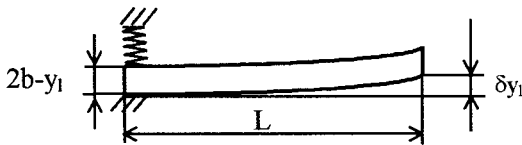
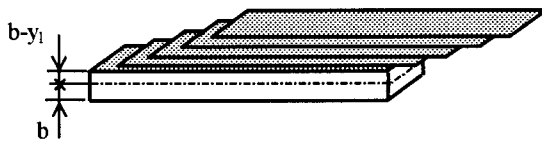
THEORETICAL

Heat Transfer Analysis

We consider here the idealized problem in which a semicrystalline polymer slab is initially at a



(a)



(b)

Figure 1 (a) Coordinate system in a freely quenched polymer slab being cooled symmetrically on both surfaces. (b) Free quenching experiment and residual stress measurement.

uniform temperature T_0 and quenched into different coolants, for example, water and air, having different coolant temperatures, T_q . As illustrated in Figure 1(a), the lateral dimensions of the slab are much larger than its thickness, $2b$. It can be assumed that during quenching, heat transfer occurs in the thickness direction y only. The cooling is symmetrical about the slab mid-plane parallel to the surfaces of the slab. At the progression of quenching, temperature gradients develop along the thickness direction of the slab. Thermal stresses are generated by the interactions between nonhomogeneous thermal contrac-

tion and changes of polymer modulus. For the purpose of determining these interactions, the variations of temperature profiles during quenching should be known. Thus, heat transfer analysis is performed. For the idealized problem stated above, a one-dimensional energy equation is given by the following²⁹:

$$\rho C_P \frac{\partial T}{\partial t} = k_{th} \frac{\partial^2 T}{\partial y^2} + \rho \dot{H}_c \quad (1)$$

where t is time; T , the temperature of the polymer; ρ , the density; C_P , the heat capacity; k_{th} , the heat conductivity; and \dot{H}_c , the heat release rate per volume due to the occurrence of crystallization during quenching, as given by

$$\dot{H}_c = X_\infty \Delta H_c \frac{\partial \theta}{\partial t} \quad (2)$$

Here, X_∞ is the ultimate degree of crystallinity for the polymer; ΔH_c , the heat of fusion for perfect crystals; θ , the relative degree of crystallinity, which is described by crystallization kinetics. The initial condition for the energy equation is

$$T|_{t=0} = T_0 \quad (3)$$

The boundary conditions are given by

$$\left. \frac{\partial T}{\partial y} \right|_{y=0} = 0 \quad (4)$$

and

$$-k_{th} \left. \frac{\partial T}{\partial y} \right|_{y=b} = h \cdot (T|_{y=b} - T_q) \quad (5)$$

where h is the heat transfer coefficient between the coolant and the polymer slab.

Crystallization and Thermal Strain

For a semicrystalline polymer, thermal contraction and the changes in mechanical properties during quenching are largely dependent upon its inherent crystallization processes, which is, in turn, related to the degree of supercooling, for example, the variation of temperature profile. To describe crystallization phenomena, nonisothermal crystallization kinetics due to Nakamura et al.^{30,31} is included. This model can be written in differential form,^{19,32} as follows:

$$\frac{\partial \theta}{\partial t} = n \cdot K(T) \cdot (1 - \theta) \cdot [-\ln(1 - \theta)]^{(n-1)/n} \quad (6)$$

where n is Avrami index; $K(T)$ is the rate constant of crystallization that is assumed to follow the Hoffman–Lauritzen expression of temperature dependence,^{19,29,32,33} as follows:

$$K(T) = (\ln 2)^{1/n} \left(\frac{1}{t_{1/2}} \right)_0 \times \exp\left(-\frac{U^*/R}{T - T_\infty}\right) \exp\left(-\frac{K_k}{T\Delta T f}\right) \quad (7)$$

with

$$\Delta T = T_m^0 - T; \quad f = \frac{2T}{T + T_m^0}; \quad T_\infty = T_g - 30$$

Here, $\left(\frac{1}{t_{1/2}}\right)_0$, a prefactor; U^* , the universal activation energy for molecular segmental jump; R , universal gas constant; K_k , nucleation exponent; ΔT is generally referred to as the degree of supercooling, which is viewed as the driving force for quiescent crystallization; T_m^0 , the equilibrium melting point of the polymer. To take into account the induction time t_I prior to the start of nonisothermal crystallization, the concept of the induction time index \bar{t} due to Sifleet et al.^{29,32,34,35} is employed. According to Chan and Isayev,³⁵ the induction period of nonisothermal crystallization is decomposed into various infinitesimal durations of time, in which isothermal crystallization is assumed. It can be written that in differential form^{29,32,35}

$$\frac{d\bar{t}}{dt} = \frac{1}{t_{qi}(T(t))} \quad (8)$$

where t_{qi} is the induction time of isothermal crystallization under temperature T . Thus, when \bar{t} reaches unity, nonisothermal crystallization is considered to start. Based upon the expression for the induction time of isothermal crystallization due to Godovsky and Slonimsky,³⁶ we have

$$t_{qi}(T) = t_m \cdot (T_m^0 - T)^{-a} \quad (9)$$

Thus, by applying eq. (9) to eq. (8), the induction time for nonisothermal crystallization t_I can be determined by solving the following integral equation:

$$\bar{t} = \int_0^{t_I} \frac{dt}{t_m \cdot [T_m^0 - T(t)]^{-a}} \equiv 1 \quad (10)$$

Subsequent to the induction period of crystallization, crystals grow from the formed nuclei. The development of crystallinity during the growth period of crystallization can be calculated using eq. (6) based on the known temperature fields from temperature analysis for quenching.

For the idealized problem of free quenching considered here, global restrictions to thermal contraction (or strain) of the polymer do not exist. However, local restrictions occur from the neighboring material elements present due to the non-homogeneous local thermal contractions arising from the existence of temperature gradients along the slab thickness direction. As a result of the continuity of materials, such local restrictions to thermal contractions produce thermal stresses in bulk. Since the polymer properties depend upon time and/or temperature, such stresses would persist in the form of residual stresses when the polymer reaches thermal equilibrium with the coolant and the crystallization is completed. To model the local thermal restrictions, the linear local thermal strain ε_{th} is defined in terms of the local specific volume V , which is obviously a function of local temperature and local degree of crystallinity. That is,

$$\varepsilon_{th}(y, t) = \frac{1}{3} \frac{V(T(y, t), \theta(y, t)) - V_0}{V_0} \quad (11)$$

where V_0 is the specific volume of the polymer at the initial temperature T_0 . For the case of free quenching, we can utilize the Spencer–Gilmore $P - V - T$ equation of state at pressure $P = 0$ for the calculation of the local specific volume^{32,37,38} under a single phase, either amorphous phase ($\theta \equiv 0$) or completely crystallized phase ($\theta \equiv 1$), according to the following linear relation:

$$V_p(T, \theta) \equiv V_p(T) = \hat{V}_p + \hat{\beta}_p T \quad (12)$$

where the subscript p ($=a$ or c) refers to amorphous ($\theta \equiv 0$) and completely crystallized phase ($\theta \equiv 1$), respectively; \hat{V}_p and $\hat{\beta}_p$ are the corresponding material constants. Typically, the $P - V - T$ curve of a semicrystalline polymer consists of a transition region and two linear regions corresponding to amorphous and completely crystallized states, respectively.^{32,37,38} The two linear regions corresponding to amorphous phase and

completely crystallized phase are well defined by fitting eq. (12) to the experimental $P - V - T$ data. For the transition region that $0 < \theta < 1$, the rule of mixture is assumed in the present study to approximate $V(T, \theta)$ at any mixed phases based on the portions of amorphous and completely crystallized phases, $V_a(T)$ and $V_c(T)$. With V_a and V_c being calculated with the fitted material parameters, we can uniformly write

$$V(T, \theta) = \theta \cdot V_c(T) + (1 - \theta) \cdot V_a(T) \quad 0 \leq \theta \leq 1 \quad (13)$$

With incorporation of eqs. (12) and (13), Equation (11) can be used to determine the varying local thermal strains during quenching. Therefore, thermal loading at a site arising from the differences in the local thermal strains of neighboring material elements can be determined for the purpose of calculating thermal stresses in the polymer.

Stress and Strain Analysis

The idealized problem of determining the thermal stress distribution in a polymer slab cooled symmetrically on both faces is similar to the one for inorganic glass considered by Muki and Sternberg,²³ and Lee et al.²⁵ Figure 1(a) shows the orientation of the coordinate axes for a polymer slab of thickness $2b$. Obviously, the symmetry of cooling demands that all shear stresses be zero. That is,

$$\sigma_{xy} = \sigma_{yz} = \sigma_{xz} \equiv 0 \quad (14)$$

Since no surface traction is acting on the faces of the slab, the normal stress in the thickness direction of y is identically equal to zero,

$$\sigma_{yy} \equiv 0 \quad (15)$$

Hence, the problem is reduced to one of planar stresses, in which the only normal stresses σ_{xx} and σ_{zz} are nonzero. As pointed out above, with lateral dimensions large compared with the thickness, these two nonzero stress components are equal, apart from a possible edge effect. Consequently, it can be written that

$$\sigma_{xx} = \sigma_{xx}(y, t) = \sigma_{zz} = \sigma_{zz}(y, t) \quad (16)$$

For convenience, $\sigma_x(y, t)$ is written for the only nonzero stress components that need be considered for the idealized free quenching problem.

Similarly, σ_y is used to represent the normal stress σ_{yy} . Since no external forces act on the lateral sides of the slab during free quenching, it is required that

$$\int_0^b \sigma_x(y, t) \equiv 0 \quad (17)$$

For strain analysis, the symmetry of cooling and material continuity across the thickness direction demand all shear strain components, including ε_{xy} , ε_{xz} , and ε_{yz} , to be zero due to the facts that the lateral dimensions are much larger than the slab thickness, and the edge effects are neglected. Among the nonzero normal strains, the strain components in the xz plane are independent of y , namely, $\varepsilon_{xx}(t) = \varepsilon_{zz}(t)$. Thus, it can be written that

$$\varepsilon_{yy} = \varepsilon_{yy}(y, t) \quad (18)$$

$$\varepsilon_{xx} = \varepsilon_{xx}(t) = \varepsilon_{zz} = \varepsilon_{zz}(t) \quad (19)$$

For convenience, ε_{xx} and ε_{zz} are referred to as ε_x , and ε_{yy} as ε_y . With the above basic stress and strain analysis for the idealized problem of free quenching, the model development for the calculation of residual thermal stresses in semicrystalline polymer is greatly simplified.

Thermoelastic Model

We first turn to discuss thermoelastic modeling of thermal stresses based on some modifications of the Indenbom theory for inorganic glasses using the instant freezing assumption.^{1,2,20,21} Accordingly, it is assumed that a crystallizing polymer is considered to be perfectly plastic before the relative degree of crystallinity θ reaches a so-called transitional value θ_c , indicating the completion of crystallization. When $\theta \geq \theta_c$, the polymer is considered to be perfectly elastic. According to the Indenbom theory,^{1,2,21} normal strain ε_x , which is independent of y as noted in the previous section, can be decomposed into three components. That is,

$$\varepsilon_x(t) = \varepsilon_e(y, t) + \varepsilon_p(y, t) + \varepsilon_{th}(y, t) \quad (20)$$

where ε_e is called elastic strain; ε_p , plastic strain. For the plastic region where $\theta(y, t) < \theta_c$ and $\varepsilon_e \equiv 0$, eq. (20) reduces to

$$\varepsilon_x(t) = \varepsilon_p(y, t) + \varepsilon_{th}(y, t) \quad (21)$$

For the elastic region, the averaged elastic strain over the region $\bar{\varepsilon}_e$ is zero. Thus, the averaged total strain $\bar{\varepsilon}_x$ takes the form,

$$\bar{\varepsilon}_x(t) = \bar{\varepsilon}_p(t) + \bar{\varepsilon}_{th}(t) \quad (22)$$

where

$$\begin{aligned} \bar{\varepsilon}_p(t) &= \frac{1}{b - y^*} \int_{y^*}^b \varepsilon_p(y, t) dy; \quad \bar{\varepsilon}_{th}(t) \\ &= \frac{1}{b - y^*} \int_{y^*}^b \varepsilon_{th}(y, t) dy \quad (23) \end{aligned}$$

where y^* is the interface between the plastic and elastic regions. It is noted that ε_x is independent of y , for example, $\varepsilon_x(t) \equiv \bar{\varepsilon}_x(t)$. Assuming that the interface y^* moves inwards regularly from the slab surface during quenching, it can be obtained from eqs. (21) and (22) that at the interface of y^* ,

$$\varepsilon_p(y^*, t) = \bar{\varepsilon}_p(t) + [\bar{\varepsilon}_{th}(t) - \varepsilon_{th}(y^*, t)] \quad (24)$$

It should be noted that the plastic strain is initially zero and increases as cooling proceeds. It becomes residual when the material element is immediately vitrified at the interface of y^* . When the whole slab is vitrified, cooling is still continued until the thermal equilibrium with the coolant is obtained. Thus, it can be attained from eqs. (20) and (22) that

$$\varepsilon_e(y) = [\bar{\varepsilon}_p - \varepsilon_p(y)] + [\bar{\varepsilon}_{th} - \varepsilon_{th}(y)] \quad (25)$$

Then, thermal stresses in the slab can be calculated by the equation of elasticity,¹

$$\sigma_x = \frac{E_e \varepsilon_e}{(1 - \nu)} \quad (26)$$

where E_e is Young's modulus of the polymer at coolant temperature; ν , Poisson ratio. Thus far, according to eqs. (24)–(26), the development of thermal stresses during quenching can be simulated. It should be pointed out that the residual plastic strains, $\varepsilon_p(y, t)$ are determined at the interface of y^* between the elastic and plastic regions. The interface is assumed to move regularly from the slab surface towards the center, dependent upon the rate of crystallization. Once

the residual plastic strains are determined, all involved calculations are straightforward.

Thermoviscoelastic Model

Thermoviscoelastic model is developed based upon the theory of linear viscoelasticity. It is of interest to note that crystallization induces phase transformation in the polymer being initially amorphous. When quenching goes on, crystalline phase appears at the expense of amorphous one. After the completion of crystallization, the fraction of the crystalline phase in terms of crystallinity remains constant. It is well recognized that mechanical and physical properties of the polymer during crystallization are strongly influenced by the development of crystallinity. To consider the effects of varying crystalline phase during quenching, we assume a simple linear rule between viscoelastic properties, such as shear relaxation modulus G and the absolute degree of crystallinity, $X (= \theta \cdot X_\infty)$. Thus, one can approximate the modulus G of the polymer having the absolute degree of crystallinity X based upon the moduli, for example, G_m and G_c , at two reference phases of different degrees of crystallinity. According to the time–temperature equivalence, it can be written that the modulus at the current time t and temperature T is

$$\begin{aligned} G(T, t) &= \frac{X(t) - X_2}{X_1 - X_2} G_1(T_r, \xi_1(t)) \\ &\quad + \frac{X(t) - X_1}{X_2 - X_1} G_2(T_r, \xi_2(t)) \quad (27) \end{aligned}$$

where $G_1(T_r, \xi_1)$ and $G_2(T_r, \xi_2)$ are the master curves of shear relaxation modulus at the reference temperature T_r for two reference phases having the absolute degrees of crystallinity of X_1 and X_2 , respectively; ξ_1 and ξ_2 are the associated reduced times defined as

$$\xi_1(T) = \int_0^t \frac{ds}{a_{T,1}(T(s))}; \quad \xi_2(T) = \int_0^t \frac{ds}{a_{T,2}(T(s))} \quad (28)$$

Here, $a_{T,1}$ and $a_{T,2}$ are the corresponding shift factors for the master curves at temperature T . For the idealized quenching cases considered in the present study, the Morland–Lee constitutive equation^{22–25} reduces to

$$\begin{aligned} \sigma_x(y, t) \equiv \sigma_z(y, t) &= \int_0^t \left\{ 2G(\xi - \xi') \cdot \frac{\partial}{\partial \tau} \right. \\ &\quad \left. \times [\varepsilon_x(\tau) - \varepsilon_y(y, \tau)] \right\} \cdot d\tau \quad (29) \end{aligned}$$

$$\sigma_y(y, t) = \int_0^t \left\{ -\frac{4}{3} G(\xi - \xi') \cdot \frac{\partial}{\partial \tau} [\varepsilon_x(\tau) - \varepsilon_y(y, \tau)] \right. \\ \left. + K(y, \tau) \cdot \frac{\partial}{\partial \tau} [2\varepsilon_x(\tau) + \varepsilon_y(y, \tau) - 3\varepsilon_{th}(y, \tau)] \right\} \cdot d\tau \quad (30)$$

where bulk modulus K is assumed to be crystallinity-dependent only. Assuming K_a and K_c are the bulk modulus values corresponding to the amorphous and completely crystallized phases, respectively, it can be written that for any relative degree of crystallinity, the bulk modulus

$$K(\theta) = \theta \cdot K_c + (1 - \theta) \cdot K_a \quad (31)$$

Based on the Boltzmann superposition principle and eq. (27), the term $G(\xi - \xi')$ in eqs. (29) and (30) is extended to the form

$$G(\xi - \xi') = \frac{X(\tau) - X_2}{X_1 - X_2} G_1(\xi_1 - \xi'_1) \\ + \frac{X(\tau) - X_1}{X_2 - X_1} G_2(\xi_2 - \xi'_2) \quad (32)$$

$$\xi_1 = \int_0^t \frac{ds}{a_{T,1}(s)}; \quad \xi'_1 = \int_0^\tau \frac{ds}{a_{T,1}(s)}; \quad \xi_2 \\ = \int_0^t \frac{ds}{a_{T,2}(s)}; \quad \xi'_2 = \int_0^\tau \frac{ds}{a_{T,2}(s)}. \quad (33)$$

Substituting eq. (29) into eq. (17) and eq. (30) into eq. (15) gives rise to a system of equations comprised of two independent equations with the two following unknowns: ε_x and ε_y . Thus, the equations can be solved, and then the nonzero thermal stress σ_x can be determined from the obtained values of ε_x and ε_y using eq. (29). Since the equations are highly nonlinear, it is difficult to find an analytical solution. A finite difference method is utilized.³⁹

EXPERIMENTAL

The polymer used in this study is a typical semicrystalline polymer, namely, isotactic polypropylene, Profax PP-6823, supplied by Himont USA, Inc. (Wilmington, DE). Its weight-averaged

molecular weight is 670,000, its melt index is 0.51 dg/min, and its polydispersity index is 3.90.²⁹

Compression molding was employed to prepare the plaque having the thickness of 3 mm. A slab cut from the plaque was heated in a thermostat oven at 180, 190, or 210°C for about 45 min and then immediately quenched into air or water at 25 or 45°C. The slab was cut into a straight bar of 50 × 6 × 3 mm. Thin layers were removed from one surface of the bar using a high-speed Tensikut milling machine with a straight trimmer.¹ The resulting imbalance of residual thermal stresses due to the layer removal causes the bar to warp to the shape of a circular arc, and the resultant curvature was quickly measured. This is illustrated in Figure 1(b). For the freely quenched polymer slab whose lateral dimensions are much larger than its thickness, the curvature of the remaining bar due to a series of layer removal φ_x is approximately calculated as a function of the overall depth of the previous layers being removed y_1 . That is,

$$\varphi_x(y_1) = \varphi_z(y_1) = \frac{2 \cdot \delta y_1}{L^2} \quad (34)$$

where L is the length of the polymer bar, and δy_1 is the displacement at the far end of the polymer bar, as illustrated in Figure 1(b) due to the warping that arises from the layer removal so far. The residual stresses can be calculated from the measured curvature as a function of the depth of material removed.^{1,2,18,28} This layer removal method for the determination of residual stresses is originally due to Treuting and Read.²⁸ According to them, the relation of residual stress to the measured curvature is

$$\sigma_{xx}(y_1) = \sigma_{zz}(y_1) = \frac{-E}{6(1 - \nu)} \left[(b + y_1)^2 \frac{d\varphi_x(y_1)}{dy_1} \right. \\ \left. + 4(b + y_1)\varphi_x(y_1) - 2 \int_{y_1}^b \varphi_x(y) dy \right] \quad (35)$$

It should be noted that only the curvature in the longitudinal direction need to be measured. This is based upon the assumption that the directional effect in the plane of the quenched samples can be neglected as $\sigma_x \equiv \sigma_z$. Otherwise, the relation of residual stresses to curvatures will become slightly more complicated.^{1,2,18,28}

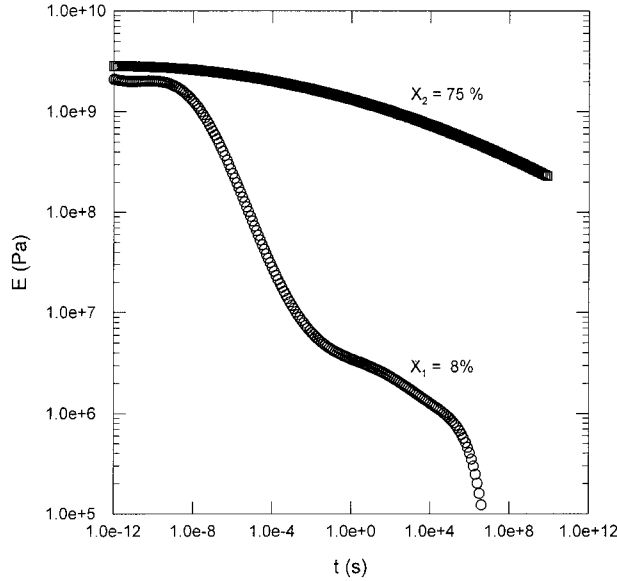


Figure 2 The master curves of Young's modulus of isotactic polypropylene at various absolute degrees of crystallinity at the reference temperature $T_r = 20^\circ\text{C}$ (data are taken from Faucher⁴²).

RESULTS AND DISCUSSION

Material Characterization

To perform temperature analysis for the simulation of free quenching, relevant physical and thermal properties of polypropylene were taken from the literature,^{29,40} as follows: the density, $\rho = 900 \text{ kg m}^{-3}$; thermal conductivity, $k_{\text{th}} = 1.93 \times 10^{-1} \text{ W/(m K)}^{-1}$; specific heat capacity, $C_P = 2.14 \times 10^3 \text{ J/(kg K)}$. In particular, a constant thermal conductivity is used in the present calculations instead of the thermal conductivity dependent upon crystallinity. As shown in 41, the use of the variable thermal conductivity has practically a little influence on temperature and spherulite size development during quenching in comparison with those based on the constant thermal conductivity. In addition, the heat transfer coefficient between the polymer and different coolants h is experimentally determined.⁴¹ It is found that $h = 350 \text{ J/(m}^2\text{K)}$ between the polymer and water, and $h = 27 \text{ J/(m}^2\text{K)}$ between the polymer and air. For the modeling of crystallization phenomena during quenching, various material parameters due to Isayev and Catignani²⁹ were utilized. This includes $t_m = 1.71 \times 10^{-17} \text{ (s K}^{10}\text{)}$; $a = 10$; $(1/t_{1/2})_0 = 1.528 \times 10^{-8} \text{ (s}^{-1}\text{)}$; $K_k = 3.81 \times 10^{-5} \text{ (K}^2\text{)}$; $n = 3$; $\Delta H_c = 9.1020 \times 10^4 \text{ (J kg}^{-1}\text{)}$, and $X_\infty = 0.4355$. For the determination of thermal loading during quenching, the material

parameters in the Spencer–Gilmore $P - V - T$ equation of state need be provided. From the literature,^{32,37,38} it is found that $\hat{V}_a = 9.225 \times 10^{-4} \text{ m}^3 \text{ kg}$; $\hat{V}_c = 9.95 \times 10^{-4} \text{ m}^3 \text{ kg}$; $\hat{\beta}_a = 8.313 \times 10^{-7} \text{ m}^3/(\text{kg K})$, and $\hat{\beta}_c = 4.284 \times 10^{-7} \text{ m}^3/(\text{kg K})$.

Various material parameters related to the mechanical properties of the polymer are required for the numerical simulations. For the thermoelastic model, Young's modulus $E_e = 1.5 \times 10^9 \text{ Pa}$ and Poisson ratio $\nu = 0.43$.⁴⁰ For the thermoviscoelastic model, the master curves of Young's modulus at two reference phases of polypropylene with the absolute degree of crystallinity, $X_m = 8\%$ and $X_c = 75\%$, at the same reference temperature, $T_r = 20^\circ\text{C}$, are adopted from Faucher,⁴² along with the corresponding shift factors: $a_{T,1}(T)$ and $a_{T,2}(T)$. These are replotted in Figures 2 and 3, where the symbols represent the digitized data from Faucher.⁴² As seen from Figure 3, two sets of shift factor data for two reference phases of polypropylene seem to collapse into one single curve within the temperature range of interest: $T > T_g (= -28^\circ\text{C}^{40})$. Thus, the two shift factor functions corresponding to the two master curves of Young's modulus are assumed to be independent of their corresponding phases. Therefore, assuming that the temperature dependence of the shift factors is of the Arrhenius type, it can be written that

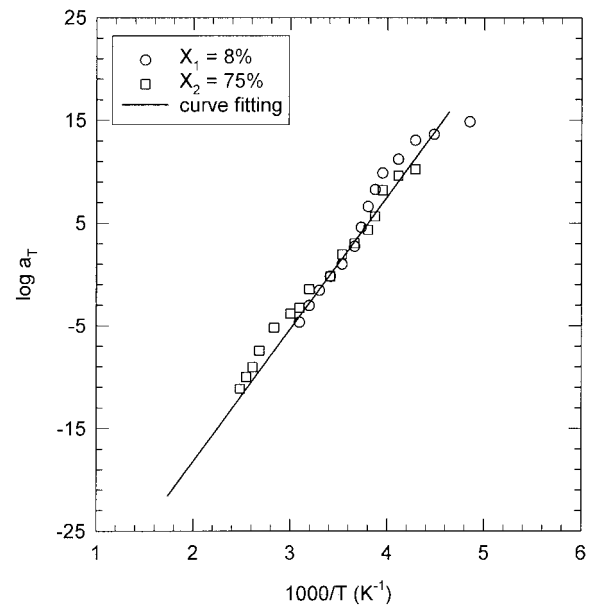


Figure 3 Shift factors versus reciprocal temperatures for iPPs at different absolute degrees of crystallinity (data are taken from Faucher⁴²). Line is according to eq. (36).

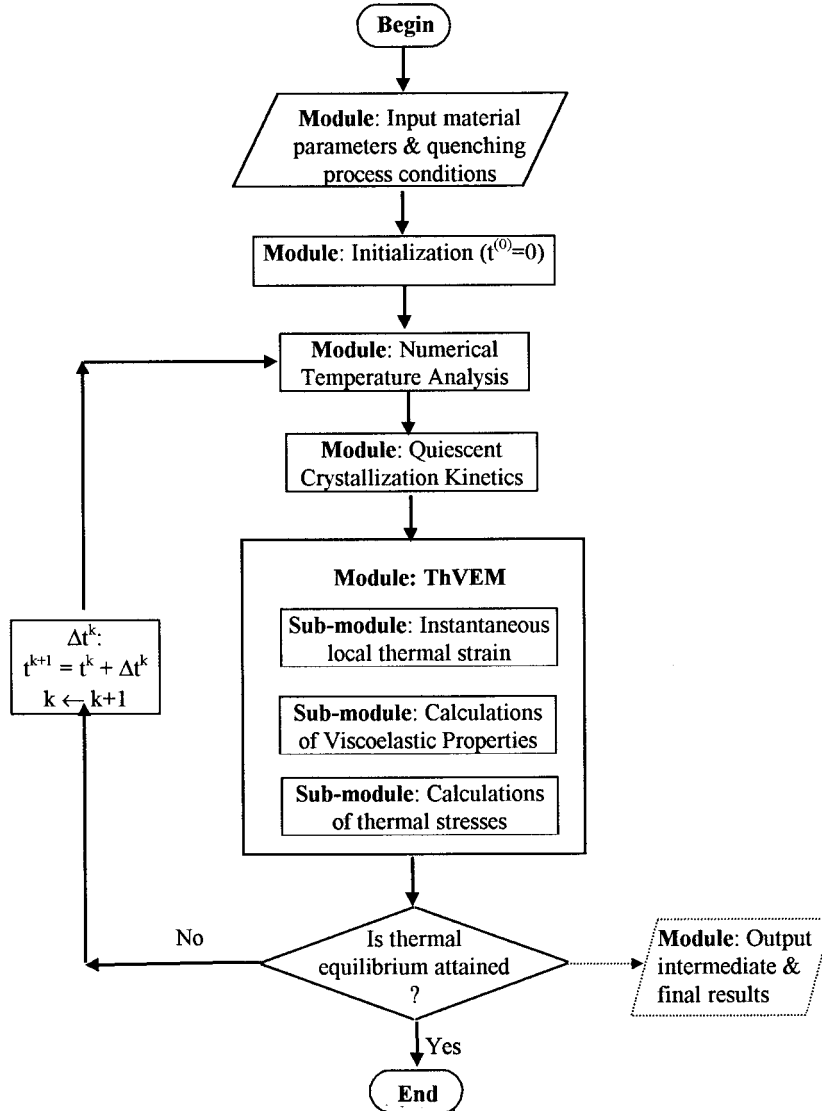


Figure 4 Numerical scheme for the process simulation of free quenching of a semi-crystalline polymer slab based upon the thermoviscoelastic model.

$$a_{T,1}(T) \cong a_{T,2}(T) = \frac{E_A}{R} \exp\left(\frac{1}{T} - \frac{1}{T_r}\right) \quad (36)$$

where E_A is termed as the activation energy. By fitting eq. (36) to the shift factor data at temperatures that $T > T_g$, as shown in Figure 3, it is found that the slope of the line fitted to the data, $\log a_T$ versus $1/T$, is 12,800 K. Therefore, the activation energy is determined to be $E_A = 244.9$ kJ/mol. Since the shear relaxation modulus, $G = \frac{E}{2(1+\nu)}$, the master curves of Young's modulus can be converted to those of shear modulus with taking $\nu = 0.5$ and 0.43 prior to and after the occurrence of crystalliza-

tion, respectively. Then, using eq. (27), the shear relaxation modulus during quenching can be evaluated. Similarly, the bulk modulus $K_a = 2.5 \times 10^9$ Pa and $K_c = 3.5 \times 10^9$ Pa⁴⁰ can be used to calculate the bulk modulus at any degree of crystallinity during quenching by using eq. (31).

Numerical Simulation

Based upon the theoretical works for the thermoelastic and thermoviscoelastic models, as discussed in the previous section, the development of temperature profile and degree of crystallinity during free quenching is determined by means of numerical temperature analysis along with crys-

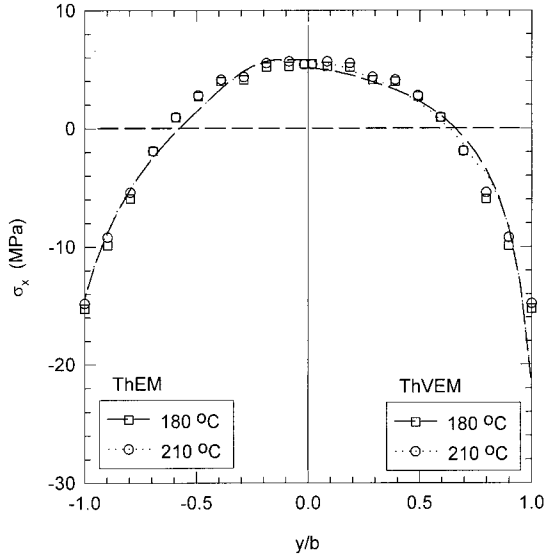


Figure 5 Thermal stress profiles for PP-6823 slabs quenched from different initial temperatures (180 and 210°C) to 25°C in water.

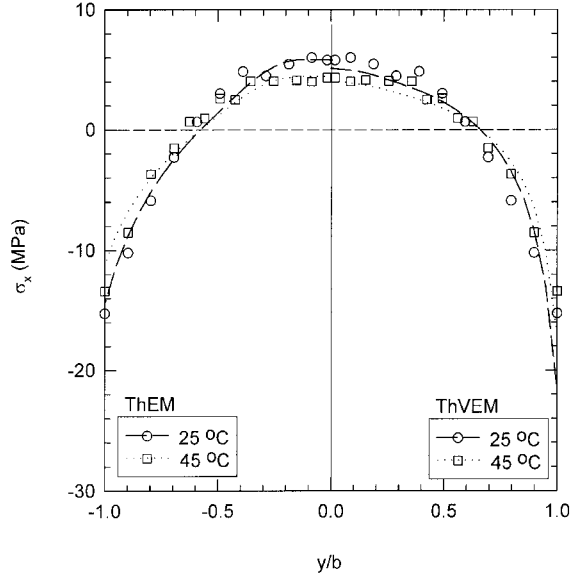


Figure 6 Thermal stress profiles for PP-6823 slabs quenched from 190°C to different coolant temperatures (25 and 45°C) in water.

tallization kinetics based upon a finite difference method. For the thermoviscoelastic model, the viscoelastic properties of the polymer need be evaluated according to eq. (27) or eq. (32). The numerical scheme is illustrated in Figure 4. It is of interest to note that the numerical simulation of free quenching of a semicrystalline polymer based upon the thermoelastic model is similar to that based upon the thermoviscoelastic model. With replacing the module: ThVEM by the module: ThEM for thermoelastic model in Figure 4, the numerical scheme for the process simulation of free quenching based on the thermoelastic model is obtained. For the simulations, 50 nodes were used to uniformly discretize the half-thickness of a slab. Simulation codes were developed using ANSI C/C++ programming language, and implemented on Silicon Graphics Personal Workstation Iris 4D/35.

Comparison of Theory with Experiments

Figures 5–7 show the predicted (lines) and measured (symbols) thermal stresses as functions of the y -locations at various quenching conditions based upon the models: ThEM and ThVEM, respectively. Generally, the predictions by both the ThVEM and ThEM agree quite well with the measurements. It is interesting to note what effect a quenching variable has on thermal stresses as predicted by the models. From Figure 5, the effect of initial polymer temperature T_0 on the stresses

can be seen. Both ThEM and ThVEM indicate that the stresses are nearly independent of T_0 . This is also verified by the experiments. The effect of the coolant temperature T_q on thermal stresses can be observed in Figure 6. Clearly, both models predict an increase in residual thermal stresses when T_q is decreased. As shown in Figure 7, different cooling media would affect the mag-

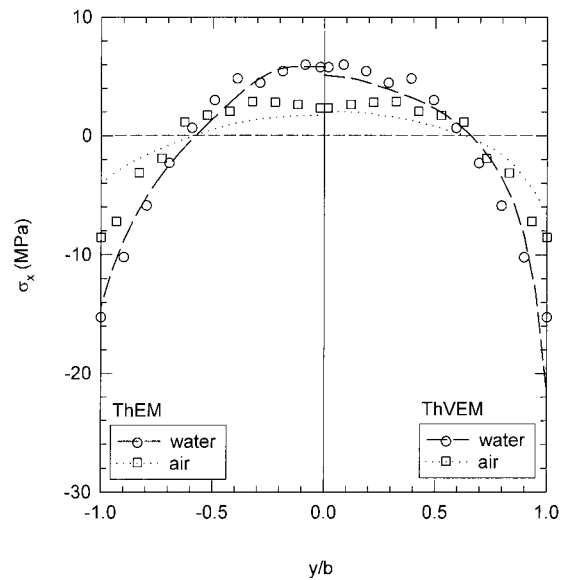


Figure 7 Thermal stress profiles for PP-6823 slabs quenched from 190 to 25°C in different cooling media (air and water).

nitude of thermal stresses. The medium having the larger heat transfer coefficient tends to induce the higher stresses. The above observations on the effects of various cooling variables can be explained by their influences upon crystallization. As known from our previous study,²⁹ the crystallization process is strongly affected by cooling conditions. The lower the coolant temperature T_q , the higher the cooling rates during the quenching. This would shorten the crystallization time in the case of PP-6823. As a result, the higher stresses get frozen in without a significant relaxation period in the molten state due to the earlier crystallization. On the other hand, initial melt temperature T_0 only very slightly affects the overall cooling rates, and the crystallization remains almost unaffected. This is because activation of crystallization is effective only after the polymer is in its supercooled state. Obviously, the more effective cooling medium introduces higher cooling rates during quenching. As a consequence, the higher thermal stresses get frozen in due to the earlier and faster crystallization. The effect of crystallization on the residual thermal stresses can be further verified by the simulations with and without the crystallization heat taken into account. Without the inclusion of crystallization heat in the simulation, the cooling rates tend to increase slightly. Thus, the predicted thermal stresses are expected to increase. This is shown in Figure 8.

In addition, the development of thermal stresses during the quenching predicted by the

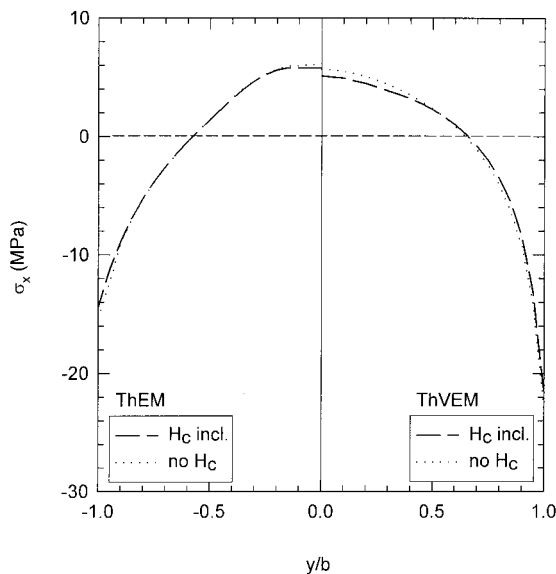


Figure 8 Thermal stress predictions for PP-6823 slab quenched from 180 to 25°C in water with and without inclusion of crystallization heat in simulations.

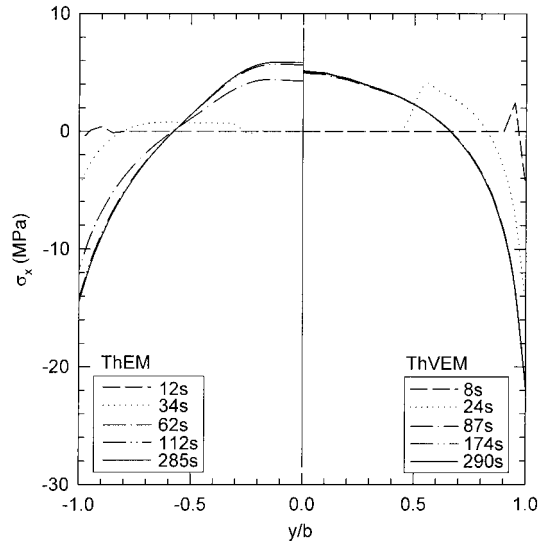


Figure 9 Transient thermal stress predictions at different cooling times in PP-6823 slab quenched from 180 to 25°C in water based on the different models.

two models is shown in Figure 9. In the earlier period of quenching, the surface layers get crystallized and contract, whereas the core layers are still in the molten state. Thus, the surface layers tend to compress the core layers, the former being in traction, but the latter being in compression. During the later period of quenching, the core layers gradually get crystallized and tend to contract. However, such contractions are hindered by the earlier frozen surface layers. As a consequence, thermal stresses herein tend to become more tensile than compressive. Finally, at the equilibrium state of quenching, thermal stresses in the core are tensile, whereas those near the surface are compressive. This has been shown by the simulations using both thermoelastic and thermoviscoelastic models.

CONCLUSIONS

Thermoelastic and thermoviscoelastic models of thermal stresses arising from free quenching of semicrystalline polymer are proposed with crystallization phenomena taken into account. It has been found that thermal stresses show a slight increase with an increase in the initial temperature of the polymer. However, coolant temperature has a significant effect on thermal stresses. Cooling medium affects the heat transfer efficiency during the quenching. This, in turn, influences the development of thermal stresses. It can

be concluded that crystallization plays a major role in governing the development of thermal stresses of a semicrystalline polymer during cooling. Faster crystallization causes higher residual stresses. The proposed models are able to provide good quantitative predictions.

REFERENCES

1. Isayev, A. I., Ed. *Injection and Compression Molding Fundamentals*; Marcel Dekker: New York, 1987.
2. Isayev, A. I.; Crouthamel, D. L. *Polym Plast Technol Eng* 1984, 22, 177.
3. Struik, L. C. E. *Polym Eng Sci* 1978, 18, 799.
4. Siegman, A.; Buchman, A.; Kenig, S. *Polym Eng Sci* 1982, 22, 560.
5. Titomanlio, G.; Drucato, V.; Kamal, M. R. *Int Polym Proc* 1987, 1, 55.
6. Wimberger-Friedl, R.; Hendriks, R. D. H. M. *Polymer* 1989, 30, 1143.
7. Kabanemi, K. K.; Crochet, M. J. *Int Polym Proc* 1992, 7, 60.
8. Wimberger-Friedl, R.; De Bruin, J. G. *J Polym Sci, Part B: Polym Phys* 1993, 31, 1041.
9. Shyu, G. D.; Isayev, A. I. *SPE Antec Tech Pap* 1993, 39, 1673.
10. Wimberger-Friedl, R.; De Bruin, J. G. *J Polym Sci* 1993, 31, 1041.
11. Flaman, A. A. M. *Polym Eng Sci* 1993, 33, 193.
12. Flaman, A. A. M. *Polym Eng Sci* 1993, 33, 202.
13. Boitout, F.; Agassant, J. F.; Vincent, M. *Int Polym Proc* 1995, 10, 237.
14. Bushko, W. C.; Stokes, V. K. *Polym Eng Sci* 1995, 35, 351.
15. Bushko, W. C.; Stokes, V. K. *Polym Eng Sci* 1995, 35, 365.
16. Bushko, W. C.; Stokes, V. K. *Polym Eng Sci* 1996, 36, 322.
17. Ghoneim, H.; Hieber, C. A. *J Therm Stresses* 1996, 19, 795.
18. Hindle, C. S.; White, J. R.; Dawson, D.; Thomas, K. *Polym Eng Sci* 1992, 32, 157.
19. Guo, X.; Isayev, A. I. *SPE ANTEC Tech Pap* 1999, 45, 1813.
20. Bartenev, G. M. *J Tech Phys* 1948, 18, 383.
21. Indenbom, V. L. *J Tech Phys* 1954, 24, 925.
22. Morland, L. W.; Lee, E. H. *Trans Soc Rheol* 1960, 4, 233.
23. Muki, R.; Sternberg, E. *J Appl Mech* 1961, 28, 193.
24. Lee, E. H.; Rogers, T. G. *J Appl Mech* 1963, 30, 127.
25. Lee, H.; Rogers, T. G.; Woo, T. C. *J Am Ceram Soc* 1965, 48, 480.
26. Narayanaawaym, O. S.; Gardon, R. *J Am Ceram Soc* 1969, 52, 554.
27. Narayanaawamy, O. S. *J Am Ceram Soc* 1978, 61, 146.
28. Treuting, R. G.; Read, W. T., Jr. *J Appl Phys* 1951, 22, 130.
29. Isayev, A. I.; Catignani, B. F. *Polym Eng Sci* 1997, 37, 1526.
30. Nakamura, K.; Watanabe, T.; Katayama, K.; Amano, T. *J Appl Polym Sci* 1972, 16, 1077.
31. Nakamura, K.; Katayama, K.; Amano, T. *J Appl Polym Sci* 1973, 17, 1031.
32. Isayev, A. I.; Chan, T. W.; Gmerek, M.; Shimojo, K. *J Appl Polym Sci* 1995, 55, 821.
33. Hoffman, J. D.; Davis, G. T.; Lauritzen, S. I. in *Treatise on Solid State Chemistry: Crystalline and Non-Crystalline Solids, Vol. 3*; Hannay, N. B., Ed.; Plenum: New York, 1976.
34. Sifleet, W. L.; Dinos, N.; Collier, J. R. *Polym Eng Sci* 1973, 13, 10.
35. Chan, T. W.; Isayev, A. I. *Polym Eng Sci* 1994, 34, 461.
36. Godovsky, Y. K.; Slonimsky, G. L. *J Polym Sci, Polym Phys Ed* 1974, 12, 1053.
37. Chiang, H. H.; Hieber, C. A.; Wang, K. K. *Polym Eng Sci* 1991, 31, 116.
38. Chiang, H. H.; Hieber, C. A.; Wang, K. K. *Polym Eng Sci* 1991, 31, 125.
39. Evens, G. A. *Practical Numerical Analysis*; Wiley: New York, 1995.
40. Krevelen, D. W. *Properties of Polymers*; Elsevier: New York, 1976.
41. de Carvalho, B.; Bretas, R. E. S.; Isayev, A. I. *J Appl Polym Sci* 1999, 73, 2003.
42. Faucher, J. A. *Trans Soc Rheol* 1959, 3, 81.